J. Synchrotron Rad. (1998). **5**, 1007–1009

XAFS in the high-energy region

Y. Nishihata,[a]* O. Kamishima,[b] Y. Kubozono,[b] H. Maeda[b] and S. Emura[c]

[a]JAERI-RIKEN SPring-8 Project Team, Kamigori, Ako-gun, Hyogo 678-12, Japan, [b]Faculty of Science, Okayama University, Okayama 700, Japan, and [c]The Institute of Scientific and Industrial Research, Osaka University, Ibaraki, Osaka 567, Japan. E-mail: yasuon@spring8.or.jp

(*Received 4 August 1997; accepted 13 November 1997*)

XAFS (X-ray absorption fine-structure) spectra were measured near *K*-absorption edges of Ce (40.5 keV), Dy (53.8 keV), Ta (67.4 keV) and Pt (78.4 keV). The blunt *K*-edge jump due to the finite lifetime of the core hole was observed. This makes it difficult to extract EXAFS (extended X-ray absorption fine-structure) functions at low k values. Local structure parameters can be evaluated from the EXAFS spectra above *K*-absorption edges in the high-energy region as well as from those above L_{III}-edges. It was found that the finite-lifetime effect of the core hole is effectively taken into the photoelectron mean-free-path term, as predicted theoretically.

Keywords: X-ray absorption fine-structure (XAFS); extended X-ray fine-structure (EXAFS); structure parameters.

1. Introduction

The radiation spectrum from a bending magnet at the SPring-8 storage ring shows sufficient photon density to observe qualitative XAFS (X-ray absorption fine-structure) spectra, even at 100 keV. This advantage makes it possible to measure XAFS spectra near *K*-absorption edges for almost all elements. XAFS spectra near L_{III}-absorption edges have been measured for heavy elements. Although the initial p state can go to final states of s or d symmetry, as an approximation the matrix element of a transition to an $l = 0$ final state is usually ignored in comparison with that of the transition to an $l = 2$ final state. EXAFS (extended X-ray absorption fine-structure) signals above most L_{III}-absorption edges are restricted to several hundred electron-volts owing to the L_{II}-absorption edge. On the other hand, there are no such assumptions and restrictions for EXAFS spectra above *K*-absorption edges. The higher an edge energy is, the easier it is to prepare a sample of uniform thickness for precise EXAFS analysis, since X-rays penetrate into thick samples in the high-energy region. However, it has been theoretically pointed out that the finite lifetime of a core hole smears out EXAFS oscillation, and that this effect becomes more serious for *K*-absorption edges of heavier elements (Stearns, 1984).

Here we report XAFS spectra observed near *K*-edges of Ce (40.5 keV), Dy (53.8 keV), Ta (67.4 keV) and Pt (78.4 keV), which were measured at the Photon Factory in the National Laboratory of High Energy Physics (KEK-PF). Local structure parameters were evaluated from EXAFS spectra above these *K*-edges and they were compared with those evaluated from EXAFS spectra above the L_{III}-edges. We discuss the effect of the lifetime broadening on the mean-free-path term of photoelectrons in the EXAFS function.

2. Experimental and analysis

We measured X-ray absorption spectra near *K*-edges of Ce (CeO_2), Dy (foil), Ta ($KTaO_3$ and foil) and Pt (foil). They were measured at beamline BL14A at KEK-PF with a vertical wiggler. Measurements were carried out at room temperature in transmission mode with an Si(553) double-crystal monochromator. The incident and transmitted X-ray intensities, I_0 and I, were monitored with a flowing Kr-gas ionization chamber 17 cm long and a flowing Xe-gas ionization chamber 31 cm long, respectively. We also measured X-ray absorption spectra of L_{III}-edges of these samples for comparison, using an EXAFS facility installed at beamline BL10B of KEK-PF. Measurements were carried out in transmission mode with an Si(311) channel-cut monochromator. The X-ray intensities were monitored with ionization chambers. The flowing gases were carefully chosen to minimize counting of the higher-order harmonics.

The energy resolution of the double-crystal monochromator in the parallel position is mainly determined by the divergence of the incident X-ray beam. The resolutions of Ce, Dy, Ta and Pt *K*-edges were estimated to be 13, 24, 37 and 50 eV, respectively, from the size of the X-ray source (1.05 mm), the width of the horizontal slit at 30 m from the centre of the vertical wiggler (1.0 mm) and the rocking curve of the monochromator crystal. The low energy resolution makes it difficult to evaluate the correct EXAFS signal especially at low k values. We did not succeed in the deconvolution of the X-ray intensities, I_0 and I, with the energy resolution function, so we avoided analysis of the EXAFS signal in the low-k region.

The programmes *XAFS93* and *MBF93* (Maeda, 1987) were employed for the data analysis to determine local structure parameters. We used an EXAFS formula for the harmonic model

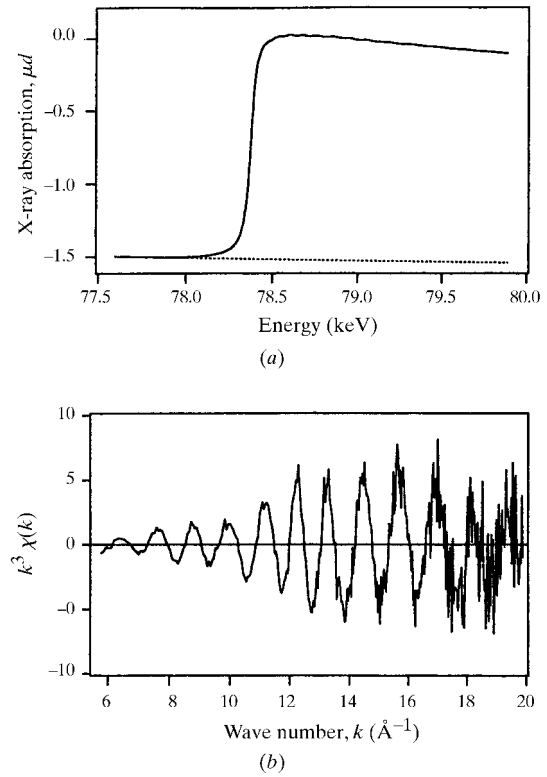

Figure 1
(*a*) XAFS spectrum near the Pt *K*-edge of Pt foil at room temperature. (*b*) EXAFS function above the Pt *K*-edge.

based on single-scattering theory and expressed by the cumulant expansion (Ishii, 1992)

$$\chi(k) = \sum_j \frac{N_j}{kR_j^2} |f_j(k,\pi)| \exp[-2\sigma_j^{(2)}k^2] \exp(-2R_j/\lambda_j) \times \sin\{2kR_j - (2k/R_j)[1 + (2R_j/\lambda_j)]\sigma_j^{(2)} + \psi_j(k)\}, \quad (1)$$

where N_j is the coordination number in the jth shell at distance R_j from the absorbing atom, $|f_j(k,\pi)|$ is the back-scattering amplitude of photoelectrons and $\psi_j(k)$ is the theoretical value of the phase shift (McKale *et al.*, 1988). The quantity $\sigma_j^{(2)}$ corresponds to the Debye–Waller factor. The wavenumber of a photoelectron is represented as $k = [2m(E - E_0)]^{1/2}/\hbar$, where m and $\hbar$ are the mass of an electron and Planck's constant, respectively. The threshold energy E_0 was assigned to an inflection point of the absorption edge. The mean free path, λ_j, of the photoelectron was taken to depend on the wavevector k with the relationship $\lambda_j = k/\eta_j$. The EXAFS function $\chi(k)$ was normalized using MacMaster coefficients. A Fourier-filtered EXAFS function concerning the first peak in real space was compared with a theoretical EXAFS function. In the parameter fitting, the theoretical EXAFS function was filtered in the same way as the observed one in order to eliminate truncation effects through the Fourier transformation of data. We used a non-linear least-squares fitting method to determine the local structure parameters.

3. Results and discussion

Fig. 1(*a*) shows the X-ray absorption spectrum near the Pt *K*-edge of Pt foil. The edge-jump of the Pt *K*-edge is not as sharp as that of the Pt L_{III}-edge shown in Fig. 2(*a*). The EXAFS signal above the Pt *K*-edge seems to smear out. As shown in Fig. 1(*b*), however, the EXAFS signal is defined well up to 18 Å^{-1}. The amplitude of the EXAFS function of the *K*-edge is considerably smaller than that of the Pt L_{III}-edge shown in Fig. 2(*b*). The width of an edge-jump is dependent on the width of the initial state of the *K*-level, Γ_K. The blunt edge-jump at the Pt *K*-edge makes it difficult to extract the EXAFS signal at low k values. In Fig. 3 the Fourier-filtered EXAFS function concerning the first nearest neighbour of the Pt *K*-edge is compared with that of the Pt L_{III}-edge. It shows clearly the phase difference of π. Table 1 gives local structure parameters of Pt and also those of the other materials. Here, R is the interatomic distance and ΔR is the difference between the interatomic distance R and that determined by X-ray diffraction. The coordination number N was fixed. Local structure parameters calculated from the spectrum of the L_{III}-edges are also tabulated. The interatomic distance and the Debye–Waller factor obtained for *K*-edges are in good agreement with those obtained for L_{III}-edges, with the exception of the parameters of the mean free path, η.

As Stearns (1984) pointed out, an EXAFS signal is theoretically generally reduced due to the short lifetime of a *K*-hole. This smearing effect behaves in a similar manner to the mean free-path term when the amplitudes and phases are assumed to be slowly

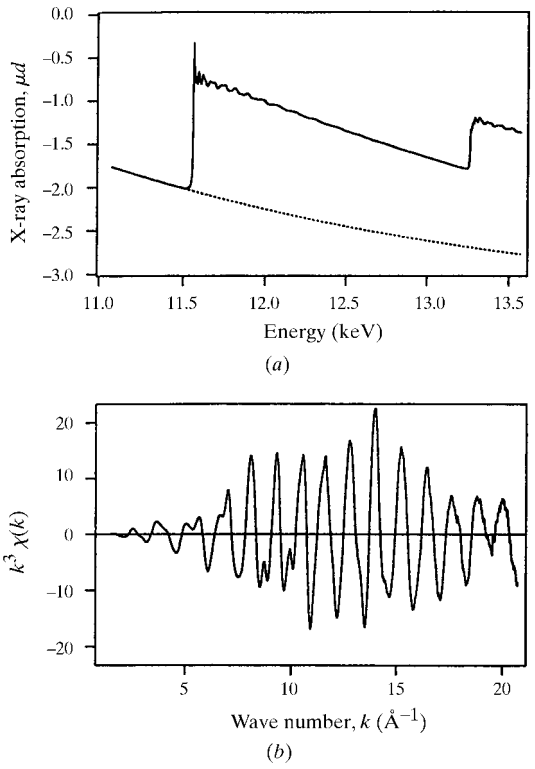

Figure 2
(*a*) XAFS spectrum near the Pt L_{III}-edge of Pt foil at room temperature. (*b*) EXAFS function above the Pt L_{III}-edge.

Table 1
Local structure parameters estimated from EXAFS spectra of *K*-edges and L_{III}-edges..

The coordination number N was fixed. ΔR is the difference of the interatomic distance R from that determined by X-ray diffraction. Some parameters, such as $\sigma^{(2)}$, η and ΔE, were calculated to be the same values for two-shell models.

Edge	N	R (Å)	ΔR (Å)	$\sigma^{(2)}$ (Å^2)	η (Å^{-2})	ΔE (eV)
CeO_2						
K	8	2.347	0.007	0.0081	1.29	−23.8
L_{III}	8	2.364	−0.006	0.0118	0.63	9.1
Dy						
K	6	3.488	−0.018	0.0071	3.03	−15.2
	6	3.586	−0.006	–	–	–
L_{III}	6	3.506	0.000	0.0134	0.91	5.4
	6	3.592	0.000	–	–	–
Ta						
K	8	2.872	0.008	0.0043	3.79	−15.5
	6	3.303	−0.004	0.0074	–	–
L_{III}	8	2.857	−0.007	0.0056	0.90	3.7
	6	3.300	−0.007	0.0079	–	–
$KTaO_3$						
K	6	1.972	−0.022	0.0069	1.82	−37.5
L_{III}	6	2.002	0.008	0.0074	0.63	15.6
Pt						
K	12	2.772	−0.002	0.0053	3.80	52.7
L_{III}	12	2.765	−0.009	0.0053	0.99	−0.3

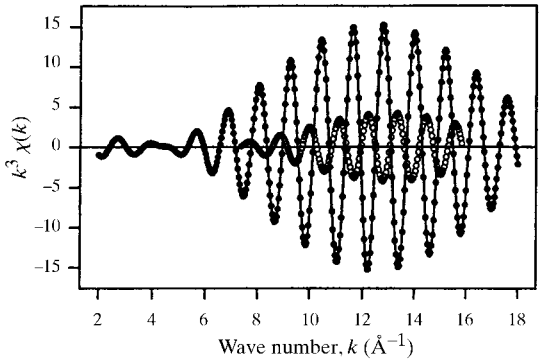

Figure 3
The Fourier-filtered EXAFS function concerning the first nearest-neighbour of the Pt *K*-edge (open circles) compared with that of the Pt L_{III}-edge (closed circles).

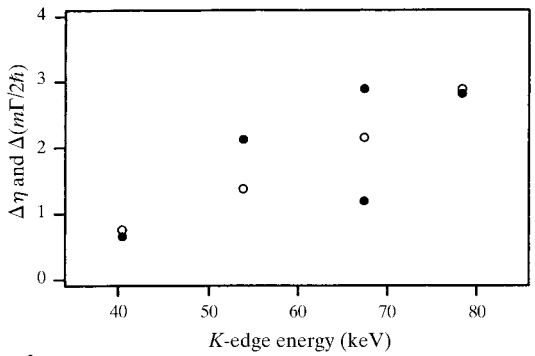

Figure 4
The difference between mean-free-path parameters, $\Delta\eta = \eta_K - \eta_{L_{III}}$ (closed circles), compared with the values of $\Delta(m\Gamma/2\hbar) = (m\Gamma_K/2\hbar) - (m\Gamma_{L_{III}}/2\hbar)$ (open circles).

varying functions of energy. The mean free path is principally modified as follows,

$$\lambda' = [(1/\lambda) + (m\Gamma_K/2\hbar k)]^{-1}. \quad (2)$$

Since the mean free path depends on the wavenumber ($\lambda = k/\eta$), we can rewrite the above equation

$$\lambda' = k/[\eta + (m\Gamma_K/2\hbar)] \quad (3)$$

$$= k/\eta'. \quad (4)$$

The influence of the finite lifetime of the core hole can be effectively taken together into η in the EXAFS function. Thus η is a good variable to examine the finite lifetime of the core hole. The large values of η for K-edges imply a short mean free path of the photoelectron. Since both the backscattering amplitude and total phase functions are monotonically decreasing functions for light atoms, the assumption described above is valid for CeO_2 and $KTaO_3$. On the other hand, since the backscattering amplitude and phase functions have peaks or valleys at the low-k region for heavy atoms, we carried out the fitting calculation using the data at the high-k region (>10 Å^{-1}) for Ta and Pt foils. Unfortunately, we had to use the data for the Dy K-edge at low k values because the signal-to-noise ratio was not good for the Dy foil. As shown in Fig. 3, the phase of the EXAFS function of the Pt K-edge swerves slightly from that of the L_{III}-edge at low k values, suggesting that the influence of the finite lifetime on the complicated back-scattering amplitude and phase functions cannot be neglected in the lower-k region. The threshold energy ΔE_0 for the fitting calculation seems to be large, as given in Table 1, because the finite lifetime effect is not considered for the theoretical values (McKale *et al.*, 1988). Fig. 4 shows the difference between the mean-free-path terms, $\Delta\eta = \eta_K - \eta_{L_{III}}$ (closed circles), estimated by the fitting analysis, as a function of the K-edge energy. Open circles represent values of $\Delta(m\Gamma/2\hbar) = (m\Gamma_K/2\hbar) - (m\Gamma_{L_{III}}/2\hbar)$, where the Γ values were taken from the literature (Krause & Oliver, 1979). The difference is an estimate of the increase in the finite lifetime effect due to the K-edge. The energy dependence of the photoelectron mean free-path term is qualitatively consistent with that of the finite lifetime of the core hole. The estimation of η depends on the range of k for the fitting calculation mainly because the low energy resolution of the monochromator reduces the amplitude of the EXAFS signal in the low-k region. For example, $\Delta\eta$ of Ta K-edge estimated from $KTaO_3$ is smaller than that estimated from Ta foil. The high-brilliance X-rays from the SPring-8 storage ring enables us to obtain XAFS spectra with higher energy resolution; energy resolution as good as 7 eV at the Pt K-edge is expected.

4. Conclusions

We have measured preliminary XAFS spectra near the K-edges of several samples in the energy region 40–80 keV. The blunt edge-jump makes it difficult to extract an EXAFS function correctly at low k values. The fitting calculation was carried out under the condition that the finite lifetime of the core hole mainly affects only the photoelectron mean-free-path term. It was found that the value of the mean-free-path term roughly corresponds to the theoretically estimated value; the mean-free-path term of the K-edge, η_K, is larger than that of the L_{III}-edge, $\eta_{L_{III}}$. Local structure parameters (with the exception of the mean-free-path term) estimated from EXAFS spectra above the K-edge are in good agreement with those estimated from EXAFS spectra above the L_{III}-edge. An XAFS study in the high-energy region at SPring-8 is scheduled in order to investigate the finite lifetime effect of the core hole.

The authors would like to thank Dr S. Kishimoto for his kind assistance in the experiment at KEK-PF.

References

Ishii, T. (1992). *J. Phys. Condens. Matter*, **4**, 8029–8034.
Krause, M. O. & Oliver, J. H. (1979). *J. Phys. Chem. Ref. Data*, **8**, 329–338.
McKale, A. G., Veal, B. W., Paulikas, A. P., Chan, S. K. & Knapp, G. S. (1988). *J. Am. Chem. Soc.* **110**, 3763–3768.
Maeda, H. (1987). *J. Phys. Soc. Jpn.* **56**, 2777–2787.
Stearns, D. G. (1984). *Philos. Mag. B*, **49**, 541–558.